Neutron scattering and magnetic studies of ferrihydrite nanoparticles

M. S. Seehra, V. S. Babu, and A. Manivannan
Department of Physics, West Virginia University, Morgantown, West Virginia 26506-6315

J. W. Lynn
NIST Center for Neutron Research, National Institute of Standards & Technology, Gaithersburg, Maryland 20899-8562

(Received 23 December 1998; revised manuscript received 16 July 1999)

Magnetic properties of two-line ferrihydrite ($FeOOD\cdot nD_2O$) nanoparticles with an average size $\simeq$4 nm are investigated using neutron scattering and magnetometry. Comparison of the neutron scattering and x-ray diffraction patterns identifies the (002) peak at $Q=1.3\,\text{Å}^{-1}$ as predominantly magnetic. The intensity of this peak, measured from 10 to 450 K, decreases almost linearly with temperature until 350 K, becoming temperature independent above 350 K. From this, $T_N\simeq 350$ K is identified to be the ordering temperature of the core spins of the nanoparticles. The width of the line is temperature independent, yielding a magnetic coherence length$\simeq$particle size. The temperature variations (5–300 K) of the initial susceptibility χ for the field-cooled (FC) and zero-field-cooled (ZFC) cases yield a peak at $T_p(m)\simeq 65$ K, below which $\chi(\text{FC})>\chi(\text{ZFC})$. For $T>T_p(m)$, the variation of χ^{-1} vs T is analyzed in terms of the model of El-Hilo *et al.*, involving particle-size distribution and interparticle interactions, and substantial interparticle interactions are inferred. Following the observations in ferritin, the field dependence of the magnetization M for $T>T_p(m)$ is analyzed in terms of the modified Langevin variation: $M=M_o\mathcal{L}(\mu_pH/kT)+\chi_aH$, where μ_p is the magnetic moment/particle. The fit at 100 K yields $\mu_p\simeq 250\,\mu_B$, consistent with the theoretical estimates based on uncompensated surface spins of Fe^{3+}.

I. INTRODUCTION

In recent years, there has been a great deal of interest in the structural and magnetic properties of ferrihydrite nanoparticles.[1–8] Ferrihydrite is a naturally occurring hydrated ferric oxyhydroxide mineral which can also be synthesized easily and is a precursor to other iron oxides such as hematite. A number of formulas have been proposed for its structure (e.g., $5Fe_2O_3\cdot 9H_2O$, $Fe_5HO_8\cdot 4H_2O$) but they are all equivalent to $FeOOH\cdot nH_2O$.[3] Generally, ferrihydrites have poor crystallinity since their x-ray-diffraction (XRD) patterns usually contain between two and six broad lines depending on the degree of crystallinity, with average particle size of 3–5 nm.[3–5] Ferrihydrite (FHYD) is also related to ferritin, an iron reservoir in living organisms, containing a ferrihydrite core encapsulated in a protein shell. Since the size of the ferritin particles can be manipulated experimentally and interparticle interactions are negligible because of the protein shell, a large number of magnetic studies dealing with the particle size effects in ferritin have been reported recently.[9–13] The small size of the FHYD nanoparticles has also been exploited for use as an adsorbent and a catalyst.[3]

For the ferrihydrite with six lines in the diffraction pattern (referred to as $6L$), the structure is known to be based on the trigonal unit cell, although the six-line XRD pattern can be equivalently indexed with a larger hexagonal cell with $a=5.08$ Å and $c=9.4$ Å.[4,5] The structures of the ferrihydrites with two lines ($2L$) and four lines ($4L$) in XRD are assumed to be similar except for lower crystalline order in the $2L$ case. Zhao *et al.*[3] have carried out a detailed analysis of the x-ray-absorption fine-structure (XAFS) spectra of $2L$ ferrihydrites. They proposed that the Fe^{3+} in the interior of the particles are coordinated by three O and three OH groups with 3.01 Å as the Fe^{3+}-Fe^{3+} separation, whereas the surface Fe^{3+} have only tetrahedral coordination. This model is in agreement with the earlier studies that showed that nearly 30% of the Fe^{3+} in these particles are tetrahedrally coordinated. The lower coordination number for the surface Fe^{3+} and the increase of their coordination number with exposure to moist air, resulting in the aggolemeration of these particles, may be due to the binding of the particles through H_2O.[3] The unsaturated surface sites are believed to be the source of the catalytic properties of these particles.[3]

The magnetic properties of the FHYD nanoparticles have been investigated by several groups using Mössbauer spectroscopy. The Mössbauer measurements by Zhao *et al.* in Ref. 1 included not only pure FHYD nanoparticles but also particles with chemisorbed SiO_4^{4-} (Si_x/FHYD with $x=\text{Si/Fe}=0.05$, 0.1, 0.15, and FHYD/SiO_2). These measurements showed that the low-temperature six-line hyperfine splitting disappeared at a superparamagnetic transition temperature $T_B(M)\simeq 100$ K and that $T_B(M)$ decreases as surface chemisorption of SiO_4^{4-} is increased for $x>0$. These results were interpreted in terms of the ''superferromagnetism'' model of Mørup *et al.*[14] in which the above $T_B(M)$ was associated with spin freezing due to interparticle interactions. Chemisorption of nonmagnetic SiO_4^{4-} reduces the interparticle interactions, resulting in a lowering of T_B.

For noninteracting nanoparticles, the time τ required to reverse the direction of magnetization is usually described by the Néel-Arrhenius relation:[15]

$$\tau=\tau_0\exp(E_a/kT). \tag{1}$$

In Eq. (1), k is the Boltzmann constant, T is the temperature and $E_a=K_aV$ is the magnetic anisotropy energy barrier be-

tween the equivalent easy axes, with K_a being the magnetic anisotropy constant and V the volume of the nanoparticles. The pre-exponential relaxation time τ_0 depends only weakly on temperature, with magnitude in the range of 10^{-9} to 10^{-13} s for various materials.[8,12] As T decreases, τ increases, and at some T the time needed for the particle magnetization to relax will exceed the characteristic time τ_c of the measurements. The blocking temperature T_B is then defined from Eq. (1) when $\tau=\tau_c$, leading to

$$T_B = E_a/k \ln(\tau_c/\tau_0). \tag{2}$$

From this relation one can calculate the blocking temperature $T_B(m)$ for dc magnetometry ($\tau_c \simeq 10^2$ s) and $T_B(M)$ for Mössbauer spectroscopy ($\tau_c \simeq 5\times 10^{-9}$ s). Using $\tau_0 = 10^{-11}$ s in Eq. (2), the ratio $T_B(M)/T_B(m) \simeq 4.8$ is obtained. The above model is found to be valid in ferritin proteins in that T_B scales appropriately with τ_c and V.[11–13] For a system with a particle size distribution, a distribution of T_B leads to the concept of an average $\overline{T_B}$,[15] which is related to the peak temperature T_p in the magnetic susceptibility by $T_p = \beta \overline{T_B}$, with $\beta \simeq 1.5$–2.0.[16,17]

Deviations of the superparamagnetic behavior from the predictions of Eqs. (1) and (2) have been observed in nanoparticles of γ-Fe_2O_3,[16–19] α-FeOOH,[20] and in ferrihydrites.[1] These deviations have been interpreted generally in terms of interparticle interactions. Investigations by El-Hilo, O'Grady, and Chantrell[17] showed that the behavior of the initial susceptibility χ for $T > T_B$ is affected by both the particle size distribution and by the interparticle dipole-dipole interaction. Their calculations showed that the temperature variation of χ follows the equation[17]

$$\chi = \frac{C}{T - T_0}, \tag{3}$$

where $T_0 (= T_i + T_b)$ has contributions from both the interparticle interaction (T_i) and a log-normal particle size distribution (T_b). At high enough temperatures, particles of all sizes are unblocked, leading to $T_0 = T_i$. However, at lower temperatures, effects of both T_i and T_b are included in the measured T_0. T_b is estimated to be negative whereas T_i is positive so that the observed χ vs T behavior in such a system for $T > T_B$ does not simply follow the Curie law expected for a superparamagnet. $T_B(m)$ and $T_B(M)$ are also affected by the interparticle dipole-dipole interaction.[21] Another factor which affects the relaxation time τ and the magnetic ground state of the nanoparticles is the microstructural details of their surfaces.[22] Thus the nature of magnetic ordering in a nanoparticle system is influenced by several factors and it remains a question of significant importance.

In this work, we report results of our investigations on the magnetism of $2L$ FHYD nanoparticles using temperature and magnetic-field variations of the magnetization M and temperature variation of a magnetic peak in neutron scattering. These studies are new since earlier magnetic studies on this system were carried out primarily by Mössbauer spectroscopy.[1–5] With $\tau_c \simeq 10^{-13}$ s (for the present energy resolution), neutron-scattering studies are ideal for determining the nature of magnetism in nanoparticles.[23–25] Our studies of $2L$ FHYD nanoparticles were undertaken to investigate the ordering temperature of the core moments, the nature of the magnetic state of the uncompensated surface moments below $T_B(m)$ and the role of interparticle interactions. Results of neutron-scattering studies presented here show that core moments order at the Néel temperature $T_N \simeq 350$ K, whereas the χ vs T gives $T_B(m) \simeq 65$ K. The observed magnetic moment $\mu_p \simeq 300\,\mu_B$/particle is shown to result from the uncompensated surface spins of Fe^{3+} and the χ^{-1} vs T behavior is analyzed in terms of the particle size distribution and interparticle interaction using the model of El-Hilo, O'Grady, and Chantrell.[17] Details of these results and their discussion are presented below.

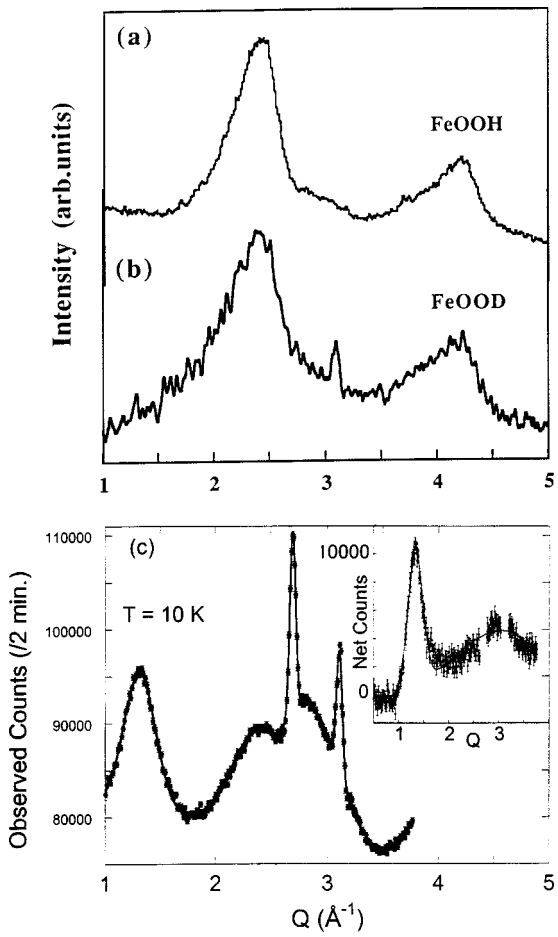

FIG. 1. Room-temperature XRD patterns of the FeOOH (a) and FeOOD (b) nanoparticles against $Q = 4\pi \sin\theta/\lambda$, the lower signal/noise in (b) being due to smaller sample. (c) Neutron-diffraction pattern of the FeOOD nanoparticles at 10 K. The inset shows the difference pattern (10 K minus 325 K) with the peaks for the Al sample holder deleted.

II. EXPERIMENTAL DETAILS

For the studies reported here, a powder sample of $FeOOH \cdot nH_2O$ was deuterated to yield a corresponding FeOOD sample, in order to reduce the background signal in neutron scattering. The procedures for preparing nanoscale $2L$ and $6L$ ferrihydrites have been described earlier.[1,3] The room-temperature XRD patterns of FeOOH and FeOOD nanoparticles (Fig. 1) show the usual two broad lines characteristic of the $2L$ ferrihydrites.[3–7] Because of lack of crys-

tallinity, these broad lines cannot be used for accurate determination of the particle size. Instead, transmission electron microscopy of this sample was carried out using the procedures outlined in Ref. 3, which gave a particle size of 40 ± 12 Å. XRD measurements of the samples were done with a Rigaku Diffractometer using CuK_α source ($\lambda \simeq 1.542$ Å). Neutron-diffraction studies were carried out at the NIST Center for Neutron Research employing neutrons of $\lambda = 2.35$ Å, with a pyrolytic graphite monochromator, analyzer, and filter and with an energy resolution of 1 meV. Studies of the sample magnetization as a function of temperature T and magnetic field H were done with a SQUID (superconducting quantum interference device) magnetometer, Quantum Design Model MPMS. The magnetization data presented here were corrected for the diamagnetic background signal from the sample holder (white plastic drinking straw). The magnetic susceptibility of this background signal is independent of magnetic field (up to 50 kOe) and temperature (5–300 K) with a magnitude of -2.3×10^{-8} emu/Oe. This represents about 1% correction to the room-temperature magnetization at 100 Oe, with decreasing contributions at lower temperatures.

III. EXPERIMENTAL RESULTS AND ANALYSIS

A. Neutron scattering and magnetic ordering

In Fig. 1, we present a comparison of the XRD patterns of the FeOOH and FeOOD samples and neutron-diffraction pattern of the FeOOD sample, in terms of momentum transfer $Q = 4\pi \sin\theta/\lambda$. The two intense broad peaks in the XRD pattern at $Q \simeq 2.4$ and 4.2 Å^{-1} and a weaker peak near $Q \simeq 3$ Å^{-1}, are similar to the observations reported by others for the $2L$ ferrihydrites.[3–7] The neutron-diffraction pattern taken at 10 K and covering the range of $Q = 0.4$ to 3.8 Å^{-1} is also shown in Fig. 1. The sharp peaks near $Q \simeq 2.7$ and 3.1 Å^{-1} are Bragg peaks due to the aluminum sample holder. The three broader peaks at $Q = 1.3$, 2.4, and 2.8 Å^{-1} are due to the FeOOD nanoparticles, the latter two essentially identical to the peaks observed in XRD. Comparison between the XRD and the neutron-diffraction patterns shows that the peak at $Q = 1.3$ Å^{-1}, observed only in the neutron-diffraction pattern, must be primarily magnetic. Referring to the hexagonal structure with $a = 5.08$ Å and $c = 9.4$ Å for the ferrihydrites, the line at $Q = 1.3$ Å^{-1} can be indexed as the (002) line of this structure. From this indexing one can infer that the chemical and the magnetic unit cells are equivalent. The fact that the (002) line does have a Bragg component as discussed later, is consistent with this interpretation.

The temperature variation of the peak at $Q = 1.3$ Å^{-1} in FeOOD was investigated from 10 to 450 K. The width of the peak was found to be temperature independent but its intensity (integrated area as well as the peak height) decreased with increase in temperature up to $T \simeq 350$ K, above which the intensity became temperature independent (Fig. 2). On heating above 425 K, the sample recrystallized to α-Fe_2O_3. The use of the Scherrer relation shows that the width of the magnetic peak is primarily due to the particle size. Since the width of the neutron peak is approximately temperature independent, this implies that the range of the magnetic order in the nanoparticle of FeOOD is temperature independent and, importantly, limited to the particle size. The importance

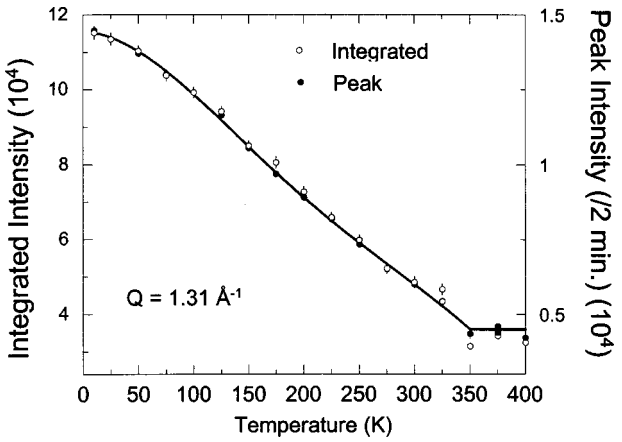

FIG. 2. Temperature variation of the intensity I (integrated and peak height) of the neutron peak at $Q = 1.3$ Å^{-1}. The line through the points is a guide to the eye.

of the above results is that for the short $\tau_c \simeq 10^{-13}$ s in neutron scattering, the individual nanoparticles of FeOOD appear magnetically ordered for $T \leqslant T_N \simeq 350$ K, with magnetic coherence length≃particle size.

The intensity I of the neutron peak is known to be proportional to the square of the order parameter. Therefore we have plotted the normalized $I_m^{1/2}$ versus T/T_N ($T_N \simeq 350$ K) after correcting for the high-temperature nuclear Bragg contribution (Fig. 3). The only known similar data is for fine particles (49 nm long by 12 nm wide) of goethite (α-FeOOH) with $T_N \simeq 358$ K (goethite has orthorhombic crystal structure),[20] and the temperature variation of $I_m^{1/2}$ for the (020) peak of goethite is also shown in Fig. 3 for comparison purposes. It is obvious that the temperature variation of the order parameter for the FeOOD nanoparticles is more rapid than goethite. This may be related to the considerably smaller size of the FeOOD nanoparticles compared to the size of the goethite, making the magnetization of FeOOD more susceptible to thermal fluctuations. A theoretical understanding of this difference is, however, lacking at present.

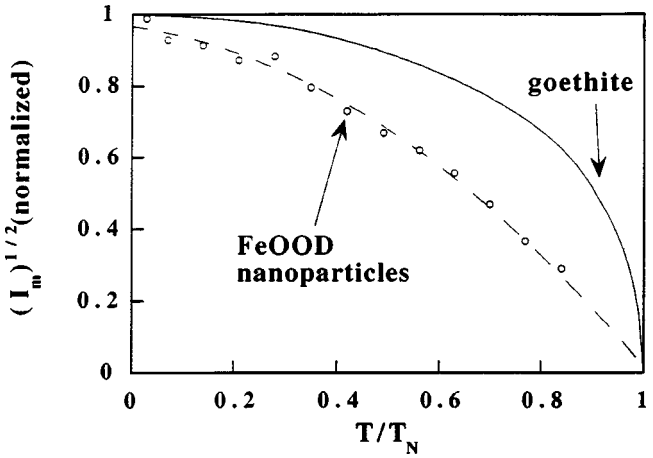

FIG. 3. Normalized $I_m^{1/2}$ versus T/T_N ($T_N = 350$ K) for the FeOOD nanoparticles where I_m is the magnetic component. For comparison, similar data for the goethite particles (α-FeOOH) is also shown from Ref. 20. The line through the points is a guide to the eye.

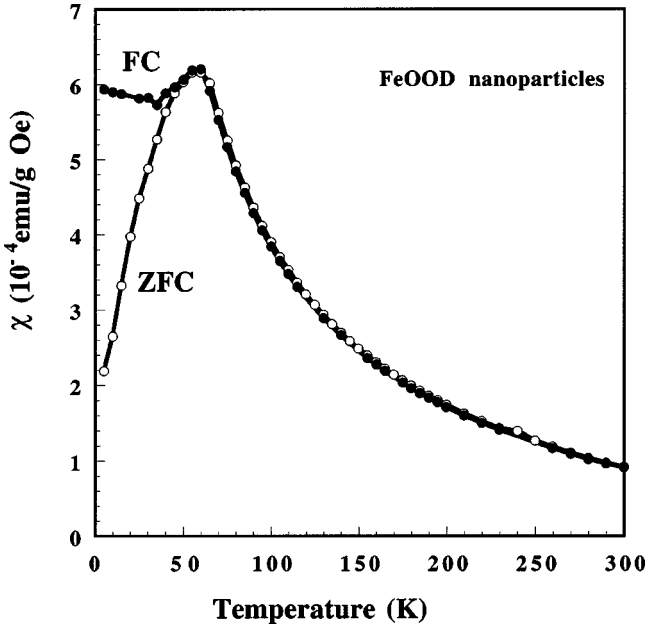

FIG. 4. Temperature variation of susceptibility $\chi = M/H$ for $H = 100$ Oe in field-cooled (FC) and zero-field-cooled (ZFC) conditions.

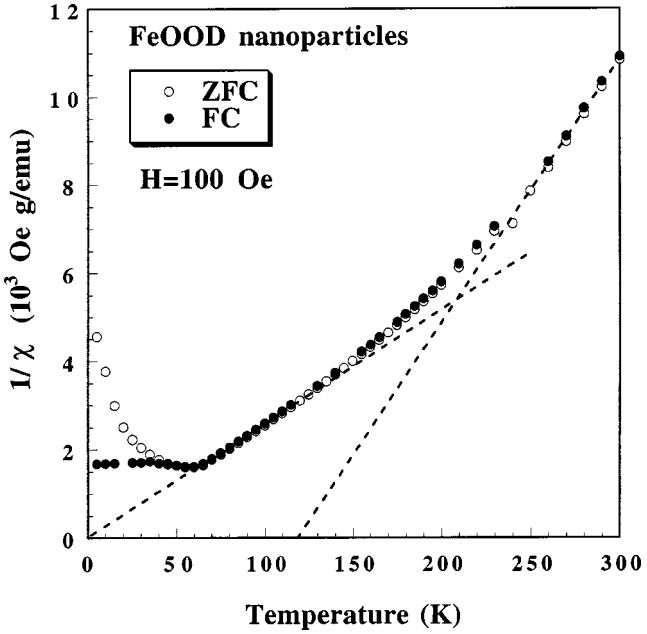

FIG. 5. Plot of χ^{-1} against T. The dotted lines represent extensions of the two linear regions explained in the text.

B. Temperature dependence of magnetic susceptibility

The temperature variation of the initial magnetic susceptibility $\chi(=M/H)$ for the FeOOD nanoparticles measured in $H = 100$ Oe, for the field-cooled (FC) and zero-field-cooled (ZFC) cases, is shown in Fig. 4. The susceptibility peaks near $T_p \simeq 65$ K, whereas the FC and the ZFC curve separate below about 50 K, similar to the observation in a commercial FeOOH nanoparticle system.[7] As noted earlier, the average blocking temperature $T_B(m)$ will usually be less than T_p because of the expected particle size distribution.[16,17]

To compare the results with Eq. (3), the χ^{-1} vs T plot is shown in Fig. 5. Following the analysis of El-Hilo, O'Grady, and Chantrell,[17] the near linear portion of the χ^{-1} vs T plot for $T > 220$ K can be associated with interparticle interactions, with $T_i \simeq 120$ K and $C_i \simeq 0.017$ emu/gOe K^{-1}. On the other hand, for the lower temperature region of $70 < T < 170$ K in Fig. 5, both progressive blocking due to particle size distribution and interparticle interactions contribute. The linearity of χ^{-1} vs T in this region yields $T_0 \simeq 0$ K and $C_0 = 0.035$ emu/gOe K^{-1}. Using $T_0 = T_i + T_b$ yields $T_b = -120$ K. Since $T_0 \simeq 0$ K, the effects of particle size distribution and interparticle interactions cancel each other in this system in the 70 to 170 K range.

The data of Fig. 4 show that below T_p, χ(FC) is nearly independent of temperature. This is in contrast to the observation in ferritin,[13] where χ(FC) continues to increase with decreasing T below T_p. Ferritin is known to be a prototypical superparamagnet[11–13] because interparticle interactions are negligible as a result of the shielding by its protein shell. So this difference in the behavior of χ(FC) below T_p (Fig. 4) warrants some discussion. In the neutron-diffraction studies reported here, an anomalous change in the scattering near $T_p \simeq 65$ K, characteristic of a phase transition, is not observed. Therefore it may be inferred that magnetic ordering of the core spins of the nanoparticles of FeOOD detected by neutron scattering below $T_N \simeq 350$ K is unaffected at T_p. However, we propose that the uncompensated surface spins with broken exchange bonds in the surface layers of the nanoparticles, which are responsible for the increase in χ with decreasing T, are affected by a cooling field. Following the arguments recently advanced by Kodama and Berkowitz,[22] the surface spins have many available configurations. A cooling field then picks out a particular spin configuration resulting in a spin-glass-type ordering of the surface spins below T_p. Because the time scale of the neutron-diffraction measurements is very short (10^{-13} s) and measurements were carried out in zero field, absence of any changes characteristics of a phase transition near $T_p \simeq 65$ K is understandable.

C. Magnetic field variation of the magnetization

The magnetization M was measured as a function of applied field H (up to 50 kOe) for several selected temperatures (100, 140, 180, 220, 260 K) above T_p. The variation of M vs H, shown in Fig. 6, is quite similar to that reported in ferritin,[13] in that this variation has a linear component, quite evident in the high H region, with a temperature-dependent susceptibility χ_a. Consequently, the Langevin variation of M expected for superparamagnetism, is modified to the equation[13]

$$M = M_0 \mathcal{L}(\mu_p H/kT) + \chi_a H. \tag{4}$$

Here μ_p is the average magnetic moment per particle, $\mathcal{L}(x) \equiv \coth x - 1/x$ is the Langevin function, M_0 is the saturation magnetization, and χ_a is the susceptibility of the antiferromagnetic nanoparticles, predicted by Néel[15] and observed, e.g., in ferritin.[13] M_0 was evaluated by extrapolating $(M - \chi_a H)$ to the limit $1/H \to 0$. The observed temperature dependence of M_0 and χ_a for the FeOOD nanoparticles are shown in Fig. 7. These temperature variations are quite simi-

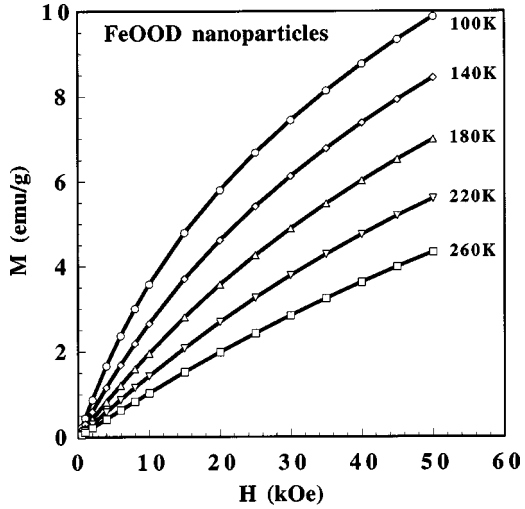

FIG. 6. Magnetization M against the applied field H at the selected temperatures indicated. The solid lines through the points are drawn as guides to the eye.

lar to those reported for ferritin,[13] although the magnitudes of M, M_0, and χ_a in FeOOD are larger by nearly an order of magnitude.

To check the Langevin variation of Eq. (4), the plot of $(M-\chi_a H)/M_0$ against H/T is shown in Fig. 8. For a temperature-independent μ_p, data at all temperatures for $T > T_p$ should collapse onto a single curve if Eq. (4) is valid. For ferritin, this was almost true in that the evaluated μ_p varied only weakly between about 300 and $360\mu_B$ for different temperatures.

For FeOOD (Fig. 8), there appears to be a consistent increase in the magnitude of μ_p with increase in temperature. We estimate magnitudes of 250, 300, 335, 360, and $400\mu_B$ at the temperatures of 100, 140, 180, 220, and 260 K respectively. This difference in the temperature variations of μ_p in ferritin and FeOOD may be due to the effects of interparticle interactions in the latter. Since the effect of the dipolar interparticle interaction is to align the uncompensated moments of the neighboring particles, this could result in the observed

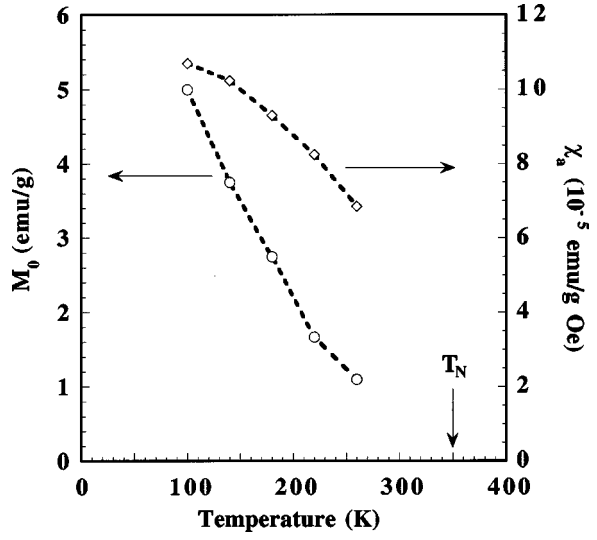

FIG. 7. Temperature variations of M_0 and χ_a of Eq. (4). The dotted lines joining the points are drawn as guides to the eye.

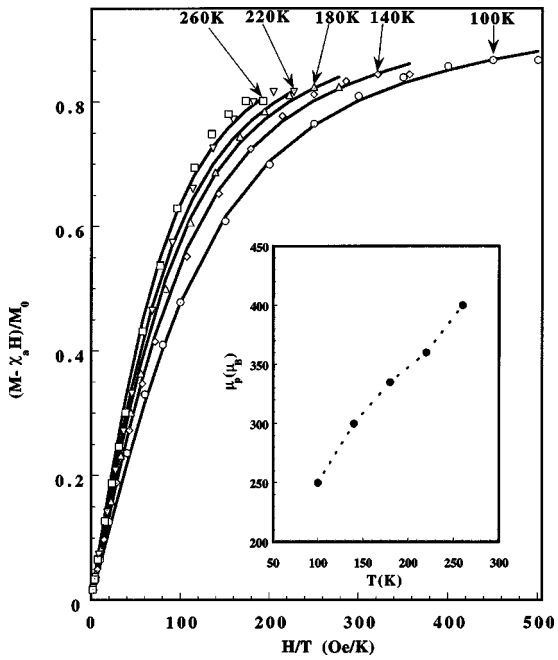

FIG. 8. Plot of $(M-\chi_a H)/M_0$ against H/T for five temperatures indicated. The solid lines represent the Langevin functions with μ_p evaluated from the fit shown in the inset at different temperatures.

increase of μ_p at higher temperatures, where the effect of this interaction is more clearly evident in the χ^{-1} vs T plot of Fig. 5. The solid lines in Fig. 8 are the Langevin function variations for different temperatures with μ_p against temperature shown in the inset of the figure. The remaining discrepancy may be associated with the particle size distribution (which will require the use of a distribution of Langevin functions) that has been ignored in the above analysis.[26]

Using the argument that the number of uncompensated surface spins approximately equals $\sqrt{N}$, where N is the total number of spins in an antiferromagnetic nanoparticle,[13,15] an estimate of μ_p can be obtained. Fe^{3+} in FeOOD are about 3 Å apart[3] and the average particle size $d \simeq 40$ Å and average particle volume $V \simeq d^3$. This yields $N \simeq 2400$/particle and so $\sqrt{N} \simeq 49$. Using $\mu = 2\sqrt{S(S+1)}\mu_B$ with $S = \frac{5}{2}$ for Fe^{3+} yields $\mu \simeq 5.9\mu_B/Fe^{3+}$ ion. This leads to $\mu_p \simeq 290\mu_B$/particle. Another estimate of μ_p can be obtained from the saturation magnetization M_0 using the relation $M_0 = \mu_p/\rho V$ where ρ and V are the density and volume of the particles, respectively. The structure of FeOOD nanoparticles is based on that of hematite for which $\rho = 5.24$ g/cm^3. For FeOOD, using $\rho \simeq 5$ g/cm^3, $M_0 \simeq 7$ emu/g obtained by extrapolating the data of Fig. 7 to $T \to 0$ K and $V \simeq d^3 = 64 \times 10^{-21}$ cm^3, we get $\mu_p \simeq 242\mu_B$. Thus the estimated magnitudes of μ_p are quite close to the experimental values determined in Fig. 8.

IV. CONCLUDING REMARKS

The results reported here for the FeOOD nanoparticles and their comparison with the observations in ferritin provides the following picture. The FeOOD particles order antiferromagnetically at $T_N \simeq 350$ K, with the temperature variation of the order parameter for $T < T_N$ significantly dif-

ferent from that in the larger goethite particles. The observed magnetization results from the uncompensated surface spins and the antiferromagnetic susceptibility of the core spins, and is affected by the interparticle interactions. The observed magnitude of the ratio $T_B(M)/T_B(m) = 100/65 \simeq 1.5$ for the FeOOD nanoparticles does not equal the predictions for an ideal superparamagnet, but it is in line with the predictions for an interacting nanoparticle system.[21] The near temperature-independent behavior of χ(FC) below $T_B(m)$ suggests that the cooling field selects a spin configuration for the surface spins which appears frozen below $T_B(m)$ on the time scale of the experiment.

ACKNOWLEDGMENTS

One of us (M.S.S.) thanks J. Zhao for assistance with the sample preparation and for useful discussions, and Diana Schwegler-Barry of NIOSH (National Institute of Safety and Health) for particle size measurements by TEM. The research at West Virginia University was supported in part by the U.S. Department of Energy (Contract Nos. DE-FC22-93PC3053 and DE-FC26-99FT40540). Identification of commercial equipment in the text is not intended to imply recommendation or endorsement by the National Institute of Standards & Technology or by West Virginia University.

[1] J. Zhao, F. E. Huggins, Z. Feng, and G. P. Huffman, Phys. Rev. B **54**, 3403 (1996).
[2] L. Cianchi, F. Gulisano, and G. Spina, J. Phys.: Condens. Matter **6**, 2269 (1994); L. Cianchi, M. Mancini, G. Spina, and H. Tang, *ibid.* **4**, 2073 (1992).
[3] J. Zhao, F. E. Huggins, Z. Feng, F. Lu, N. Shah, and G. P. Huffman, J. Catal. **143**, 499 (1993); Z. Feng, J. Zhao, F. E. Huggins, and G. P. Huffman, *ibid.* **143**, 510 (1993); J. Zhao, F. E. Huggins, Z. Feng, and G. P. Huffman, Clays Clay Miner. **42**, 737 (1994).
[4] Z. A. Pankhurst and R. J. Pollard, Clays Clay Miner. **40**, 268 (1992); J. Phys.: Condens. Matter **5**, 8487 (1993).
[5] R. A. Eggleton and R. W. Fitzpatrick, Clays Clay Miner. **36**, 111 (1998); **38**, 335 (1990).
[6] E. Murad, L. H. Bowen, G. J. Long, and T. G. Quin, Clay Miner. **23**, 161 (1988); E. Murad, J. Magn. Magn. Mater. **74**, 153 (1988).
[7] M. M. Ibrahim, G. Edwards, M. S. Seehra, B. Ganguly, and G. P. Huffman, J. Appl. Phys. **75**, 5873 (1994).
[8] M. M. Ibrahim, S. Darwish, and M. S. Seehra, Phys. Rev. B **51**, 2955 (1995).
[9] F. C. Meldrum, B. R. Heywood, and S. Mann, Science **257**, 522 (1992).
[10] T. Douglas, D. P. E. Dickson, S. Betteridge, J. Charnock, C. C. Garner, and S. Mann, Science **269**, 54 (1995).
[11] S. Gider, D. D. Awschalom, T. Douglas, S. Mann, and M. Chaparala, Science **268**, 77 (1995).
[12] S. H. Kilcoyne and R. Cywinski, J. Magn. Magn. Mater. **140-144**, 1466 (1995); see also, D. P. E. Dickson, N. M. K. Reid, C. Hunt, H. D. Williams, M. El-Hilo, and K. O'Grady, *ibid.* **125**, 345 (1993).
[13] S. A. Makhlouf, F. T. Parker, and A. E. Berkowitz, Phys. Rev. B **55**, R14 717 (1997).
[14] S. Mørup, M. B. Madsen, J. Franck, J. Villadsen, and C. J. W. Koch, J. Magn. Magn. Mater. **40**, 163 (1983); S. Mørup, Hyperfine Interact. **90**, 171 (1994).
[15] L. Néel, C. R. Hebd. Seances Acad. Sci. **252**, 4075 (1961); **253**, 9 (1961); **253**, 203 (1961); **253**, 1286 (1961).
[16] J. I. Gittelman, B. Abeles, and S. Bozoeski, Phys. Rev. B **9**, 3891 (1974).
[17] M. El-Hilo, K. O'Grady, and R. W. Chantrell, J. Magn. Magn. Mater. **114**, 295 (1992); **117**, 21 (1992).
[18] J. L. Dormann and D. Fiorani, J. Magn. Magn. Mater. **140-144**, 415 (1995); R. Zysler, D. Fiorani, J. L. Dormann, and A. M. Testa, *ibid.* **133**, 71 (1994).
[19] S. Mørup, F. Bødker, P. Hendriksen, and S. Linderoth, Phys. Rev. B **52**, 287 (1995).
[20] S. Bocquet and S. J. Kennedy, J. Magn. Magn. Mater. **109**, 260 (1992); S. Bocquet, R. J. Pollard, and J. D. Cashion, Phys. Rev. B **46**, 11 657 (1992).
[21] S. Mørup, Europhys. Lett. **28**, 671 (1994); S. Mørup and E. Tronc, Phys. Rev. Lett. **72**, 3278 (1994).
[22] R. H. Kodama and A. E. Berkowitz, Phys. Rev. B **59**, 6321 (1999).
[23] M. F. Hansen, F. Bødker, S. Mørup, K. Lefmann, K. N. Clausen, and P.-A. Lindgard, Phys. Rev. Lett. **79**, 4910 (1997).
[24] F. Gazeau, E. Debois, M. Hennion, R. Perzynski, and Yu. Raikher, Europhys. Lett. **40**, 575 (1997).
[25] D. Lin, A. C. Nunes, C. F. Majkrzak, and A. E. Berkowitz, J. Magn. Magn. Mater. **145**, 343 (1995).
[26] M. M. Ibrahim, J. Zhao, and M. S. Seehra, J. Mater. Res. **7**, 1856 (1992).